



**HAL**  
open science

# Pyranopterin Related Dithiolene Molybdenum Complexes as Homogeneous Catalysts for CO<sub>2</sub> Photoreduction

Thibault Fogeron, Pascal Retailleau, Lise-Marie Chamoreau, Yun Li, Marc  
Fontecave

► **To cite this version:**

Thibault Fogeron, Pascal Retailleau, Lise-Marie Chamoreau, Yun Li, Marc Fontecave. Pyranopterin Related Dithiolene Molybdenum Complexes as Homogeneous Catalysts for CO<sub>2</sub> Photoreduction. *Angewandte Chemie*, 2018, 130 (52), pp.17279-17283. 10.1002/ange.201809084 . hal-02298428

**HAL Id: hal-02298428**

<https://hal.sorbonne-universite.fr/hal-02298428v1>

Submitted on 26 Sep 2019

**HAL** is a multi-disciplinary open access archive for the deposit and dissemination of scientific research documents, whether they are published or not. The documents may come from teaching and research institutions in France or abroad, or from public or private research centers.

L'archive ouverte pluridisciplinaire **HAL**, est destinée au dépôt et à la diffusion de documents scientifiques de niveau recherche, publiés ou non, émanant des établissements d'enseignement et de recherche français ou étrangers, des laboratoires publics ou privés.

# Pyranopterin Related Dithiolene Molybdenum Complexes as Homogeneous Catalysts for CO<sub>2</sub> Photoreduction

Thibault Fogeron,<sup>[a]</sup> Pascal Retailleau,<sup>[b]</sup> Lise-Marie Chamoreau,<sup>[c]</sup> Yun Li<sup>\*[a]</sup> and Marc Fontecave<sup>\*[a]</sup>

**Abstract:** Two original dithiolenes, with a pyrazine ring fused with a pyran ring carrying the dithiolene chelate, mimicking molybdopterin (MPT) present in the active site of formate dehydrogenases (FDHs), have been synthesized. The first one mimicks MPT in the dihydropyrazine form while the second mimicks MPT in the more biologically relevant tetrahydropyrazine form. Both have been structurally characterized as a ligand within a Co(cyclopentadienyl)(dithiolene) complex. The corresponding MoO(dithiolene)<sub>2</sub> complexes have been also prepared and are reported as the first functional and stable catalysts inspired by the Mo center of FDHs so far: they indeed catalyze the photoreduction of CO<sub>2</sub> into formic acid, as the major product, and carbon monoxide, achieving more than 100 turnover numbers in about 8 h.

Conversion of CO<sub>2</sub> into formic acid is one of the possible strategies to store renewable energies in the form of chemical energy and to use CO<sub>2</sub> as a source of carbon. Formate has wide industrial applications and is seen as valuable within fuel cell technologies.<sup>1</sup> CO<sub>2</sub>/HCOOH interconversion is a biological reaction catalyzed by formate dehydrogenases (FDHs) whose active site might serve as a unique source of inspiration in order to design new molecular catalysts for CO<sub>2</sub> conversion to formic acid. Intriguingly, nature has exclusively selected Mo/W mononuclear centers in which the metal ion is chelated by two identical dithiolene ligands, called molybdopterin (MPT) (Figure 1).<sup>2</sup> The natural complex found in FDHs has never been isolated due to fast decomposition and synthetically mimicking it is highly challenging.<sup>3</sup> Therefore, with a few exceptions,<sup>4</sup> only simple dithiolene ligands have been used to prepare Mo/W-dithiolene complexes<sup>5</sup> and, to our knowledge, there is no example of a Mo/W-dithiolene complex reported as a catalyst for electro- and/or photo-reduction of CO<sub>2</sub> so far.

In a quest for mimicking MPT, we have previously reported an original dithiolene ligand qpdt in its protected form **1** (Figure 2) and used it to synthesize molecular Mo, Co and Ni bioinspired complexes.<sup>6</sup> While the Mo and Co complexes were found to be catalysts for H<sup>+</sup> reduction, the Ni complex was reported as a catalyst for CO<sub>2</sub> electroreduction into formic acid as the major product. However, a major drawback of qpdt-based complexes is the reactivity of the ligand under reductive conditions in the presence of protons,<sup>6d</sup> implying that these complexes are pre-catalysts rather than true catalysts.

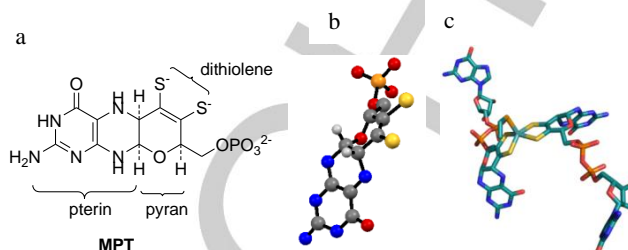


**Figure 1.** MPT: (a) Chemical representation; (b) 3D structure; (c) Mo<sup>IV</sup>(MPT)<sub>2</sub> center of the active site of FDHs with a selenocysteine axial ligand (source : PDB file 1KQF)<sup>7</sup>.

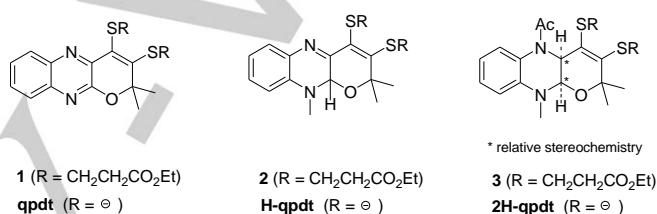


**Figure 2.** Structures of the central cycle oxidized ligand qpdt, 2-electron reduced ligand H-qpdt and 4-electron reduced ligand 2H-qpdt in the protected form **1**, **2** and **3**.

The major difference between qpdt and MPT resides in the oxidation state of the central pyrazine ring: it is fully reduced in MPT and fully oxidized in qpdt. While the tetrahydro quinonoid oxidation state is present in most cases, some enzymes have been shown to contain a MPT ligand in the dihydropyranopterin form.<sup>8</sup> In order to study biomimetic dithiolene ligands more biologically relevant to MPT than qpdt and more stable, we report here two original ligands derived from qpdt, with the central pyrazine ring either in the two-electron or the four-electron reduced state, named H-qpdt and 2H-qpdt in the protected form **2** and **3** respectively (Figure 2). The corresponding Co-cyclopentadienyl and Mo-oxo complexes were synthesized and structurally characterized. A bioinspired Mo-dithiolene complex is reported for the first time as a catalyst for the photoreduction of CO<sub>2</sub> into HCOOH and CO.

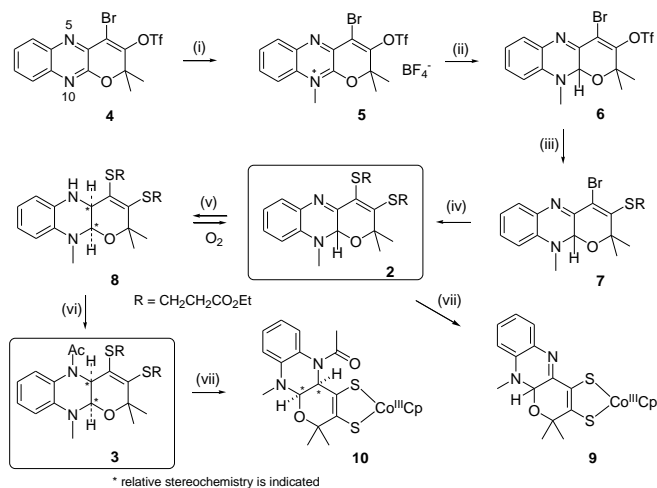
Since direct reduction of qpdt without pyran ring opening proved unsuccessful, the synthetic strategy outlined in Scheme 1 was developed, starting with the previously reported bromo-vinyl-triflic derivative **4**.<sup>6a, b</sup> In order to activate imine groups and to avoid pyran ring opening during reduction, N-methylation was carried out using trimethyloxonium tetrafluoroborate. This reaction proved highly selective: only N10 atom was methylated leading quantitatively to **5**. The reduction of the iminium group was performed with Me<sub>4</sub>NBH(OAc)<sub>3</sub> to give **6**. Then we introduced the dithiolene moiety into **6** with two Pd-catalyzed cross-coupling reactions to afford **2** in 27% yield. Further reduction of **2** gave **8**, which slowly re-oxidized to **2** in air. In order to protect the secondary amine in **8**, an acetylation was achieved to give the 4-electron reduced dithiolene ligand 2H-

[a] Dr. T. Fogeron, Dr. Y. Li, Prof. M. Fontecave  
Laboratoire de Chimie des Processus Biologiques, UMR 8229  
CNRS, Collège de France, Université Paris Sorbonne, 11 Place  
Marcelin Berthelot, 75231 Paris Cedex 05, France.  
E-mail: yun.xu-li@college-de-france.fr; marc.fontecave@college-  
de-france.fr

[b] P. Retailleau  
Institut de Chimie des Substances Naturelles, CNRS UPR 2301,  
Université Paris-Saclay, 1, av. de la Terrasse, 91198 Gif-sur-  
Yvette, France

[c] L.-M. Chamoreau  
Sorbonne Universités, Université Paris Sorbonne, Institut Parisien  
de Chimie Moléculaire, UMR 8232 CNRS, 4 place Jussieu, 75252  
Paris Cedex 5, France

qpdt in its protected form **3** (Scheme 1). A NOESY experiment showed that the two protons of the junction of the two cycles adopt a *cis* configuration. This is interesting since these two protons, in MPT, are also *cis*-oriented with *R, R* absolute configuration (Figure 1). Thus, we have succeeded in synthesizing the first ligand that displays a high degree of similarity with molybdopterin (MPT, Figure 1).



**Scheme 1.** Synthesis of dithiolene ligands **2**, **3** and CoCp(dithiolene) complexes **9**, **10**. Conditions: i)  $(\text{Me}_3\text{O})(\text{BF}_4)$ ; ii)  $\text{Me}_4\text{NBH}(\text{OAc})_3$ ; iii)  $\text{Pd}(\text{dba})_2$  (10 %), Xantphos (10 %),  $\text{HSCH}_2\text{CH}_2\text{CO}_2\text{Et}$ ,  $i\text{Pr}_2\text{NEt}$ ; iv)  $\text{Pd}_2(\text{dba})_3$  (15 %), Xantphos (30 %),  $\text{HSCH}_2\text{CH}_2\text{CO}_2\text{Et}$ ,  $i\text{Pr}_2\text{NEt}$ ; (v)  $\text{NaBH}_3(\text{CN})$ ,  $\text{AcOH}$ ; (vi)  $\text{AcCl}$ ,  $i\text{Pr}_2\text{NEt}$ ; (vii)  $\text{CoCpI}_2(\text{CO})$ .

$\text{Co}^{\text{III}}\text{Cp}(\text{dithiolene})$  complexes are known as very practical tools for structural and functional characterization of dithiolene ligands because of their diamagnetism and stability in air.<sup>9</sup> The neutral complex  $[\text{Co}^{\text{III}}\text{Cp}(\text{H-qpdt})]$  (**9**) was synthesized in a classical way: compound **2** was treated with *t*-BuOK anaerobically leading to H-qpdt. Without purification, the latter was then reacted with  $\text{CoCpI}_2(\text{CO})$ <sup>10</sup> to afford complex **9** as a green solid, in 66% yield after purification by chromatography over silica (Scheme 1). The same procedure was applied to **3** resulting in complex  $[\text{Co}^{\text{III}}\text{Cp}(2\text{H-qpdt})]$  (**10**) in 88% yield as a purple solid.

Single crystals suitable for X-ray diffraction were obtained for both complexes. A summary of the crystal data collection and refinement parameters are listed in Table S2. Selected interatomic bond lengths and angles are listed in Table S3. Complex **9** contains a chiral center and is thus a *R/S* racemic mixture (Figure S4). Complex **10** contains two chiral centers with *cis* relative configuration and is a *R,R/S,S* racemic mixture (Figure S4). The two enantiomers of complex **9** and the two enantiomers of complex **10** have been structurally characterized (Figure S4), but only one of each complex is shown in Figure 3. The structures of the two complexes are reminiscent of other previously reported  $\text{CoCp}(\text{dithiolene})$  complexes.<sup>11, 12</sup>

The <sup>1</sup>H NMR spectra of complex **9** and complex **10** in  $\text{CDCl}_3$  are shown in Figure S6. The chemical shifts reflect the electron donating character of the ligands. For example the protons of the Cp ligand are found at 5.43 ppm for complex **9** and 5.26 ppm for complex **10**, consistent with the ligand in **10** being more electron donating than that in **9**. The same trend was also observed in cyclic voltammograms (CVs): the  $\text{Co}^{\text{III}}/\text{Co}^{\text{II}}$  reduction

wave was observed at  $-0.59$  V for **9** and at  $-0.72$  V vs  $\text{Ag}/\text{AgCl}$  for **10**.

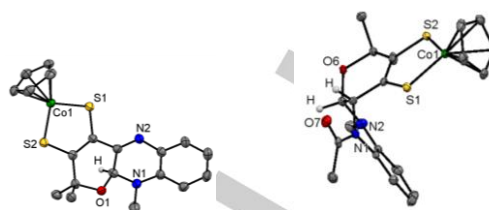
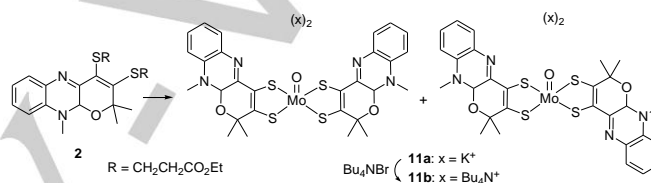


**Figure 3.** Structures and ORTEP representations of  $[\text{Co}^{\text{III}}\text{Cp}(\text{H-qpdt})]$  (**9**, left, *S*-configuration) and  $[\text{Co}^{\text{III}}\text{Cp}(2\text{H-qpdt})]$  (**10**, right, *R,R* configuration). Some hydrogen atoms are omitted for clarity.

For the preparation of  $\text{Mo}^{\text{IV}}\text{O}(\text{dithiolene})_2$  complexes **11** (scheme 2), compound **2** was deprotected and treated with  $\text{K}_3\text{Na}[\text{MoO}_2(\text{CN})_4] \cdot 6\text{H}_2\text{O}$ <sup>13</sup> under alkaline conditions at  $45$  °C for 30 min.<sup>13c</sup>



**Scheme 2.** Synthesis of *cis*- and *trans*- $[\text{Mo}^{\text{IV}}\text{O}(\text{H-qpdt})_2]^{2-}$  (**11**). Conditions: 1)  $i\text{tBuOK}$ ; 2)  $\text{K}_3\text{Na}[\text{Mo}^{\text{IV}}\text{O}_2(\text{CN})_4] \cdot 6\text{H}_2\text{O}$ ,  $\text{NaOH}$ .

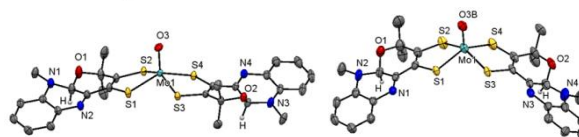
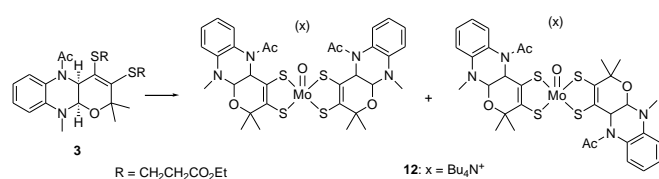


**Figure 4.** Crystal structure of the dianion of **11a** with 50% probability of ellipsoids drawing. Some hydrogen atoms are omitted for clarity. Three isomers are isolated: *trans*-*S,S* (left), *trans*-*R,R* (Figure S8) and *cis*-*S,R* (right).

Single crystals of the water soluble complex  $\text{K}_2[\text{Mo}^{\text{IV}}\text{O}(\text{H-qpdt})_2]$  (**11a**) were obtained as orange plates by layering an acetone solution of the crude product with  $\text{Et}_2\text{O}$  in a glove box. The molecular structures of the anion component  $[\text{Mo}^{\text{IV}}\text{O}(\text{H-qpdt})_2]^{2-}$  are shown in Figure 4. A summary of the crystal data collection and refinement parameters are listed in Table S4. Selected interatomic bond lengths and angles are listed in Table S5. Two different crystals were obtained. Figure 4 (left) shows the crystal structure of one enantiomer (*trans*-*S,S*) of complex **11a**, in which the two ligands are in a *trans* orientation with respect to  $\text{MoS}_4$  core. The second enantiomer is shown in Figure S8. Figure 4 (right) shows the structure of **11a** in which the two ligands are *cis*-oriented. Reported structures of  $[\text{Mo}^{\text{IV}}\text{O}(\text{dithiolene})_2]$  with *cis* isomers are rare<sup>14</sup> and such complexes generally adopt a *trans* configuration. To the best of our knowledge, it is the first time that both *cis* and *trans* isomers are structurally characterized for the same  $\text{MoO}(\text{dithiolene})_2$  complex. It is interesting to note that acetone and water molecules contribute to the crystal lattice through interactions with the  $\text{K}^+$  ions, which are also linked to the sulfur atoms and to the oxo ligands of the Mo center (Figure S9). For practical

reasons, spectroscopic characterization was achieved with the same complex having  $\text{Bu}_4\text{N}^+$  as the counter-cation (**11b**) (scheme 2). Complex **11b** is soluble in common solvents yielding orange solutions that are highly sensitive to air. Its UV/Vis absorption spectrum in  $\text{CH}_3\text{CN}$  is shown in Figure S10. The  $\nu(\text{Mo}=\text{O})$  stretch at  $901\text{ cm}^{-1}$  is similar to the one reported for  $\text{Mo}^{\text{IV}}\text{O}(\text{C}_2\text{S}_2\text{COOMe}_2)_2$ .<sup>15</sup> The negative-ion electrospray mass spectrum in acetonitrile solution exhibits a peak cluster at  $m/z = 694$ , consistent with the molecular formula (Figure S11). Complex **11** is diamagnetic and its  $^1\text{H}$  NMR spectrum shows a mixture of *cis* / *trans* isomers at an approximate 50:50 ratio (Figure S12), consistent with structural data. The CV in  $\text{CH}_3\text{CN}$  displays a reversible wave at  $-0.34\text{ V}$  (vs. Ag / AgCl) corresponding to the  $\text{Mo}^{\text{IV}} / \text{Mo}^{\text{V}}$  couple, as well as a quasi-reversible wave at  $+0.4\text{ V}$  assigned to the  $\text{Mo}^{\text{V}} / \text{Mo}^{\text{VI}}$  oxidation process (Figure S13).



**Scheme 3.** Synthesis of *cis*- and *trans*- $[\text{Mo}^{\text{V}}\text{O}(\text{2H-qpdt})_2]^-$  (**12**). Conditions: 1)  $\text{tBuOK}$ ; 2)  $\text{K}_3\text{Na}[\text{Mo}^{\text{IV}}\text{O}_2(\text{CN})_4] \cdot 6\text{H}_2\text{O}$ ,  $\text{NaOH}$ ; 3)  $\text{Bu}_4\text{NBr}$ .

Synthesis of  $[\text{Mo}^{\text{V}}\text{O}(\text{2H-qpdt})_2]^-$  (**12**) using 2H-qpdt ligand was carried out under the same conditions as for **11**. Conventional counter-ions ( $\text{K}^+$ ,  $\text{CH}_3\text{N}^+$ ,  $\text{Et}_4\text{N}^+$ ,  $\text{Bu}_4\text{N}^+$  and  $\text{Ph}_4\text{P}^+$ ) were used for crystallization. Despite many attempts, we failed to obtain single crystals suitable for x-ray diffraction. This might be due to the presence of many stereoisomers in **12**. Indeed, since 2H-qpdt exists in the form of a mixture of two enantiomers and the two ligands could be *cis* or *trans* oriented as in **11**, a mixture of seven stereoisomers was expected for **12**. We had thus to rely on a combination of different spectroscopic techniques to characterize complex **12** and to confirm the structure shown in Scheme 3.

The negative-ion electrospray mass spectrum of **12** in  $\text{CH}_3\text{CN}$  (Figure S14), with a peak cluster at  $m/z = 782$ , as well as the results of elemental analysis (see the experimental section) support the molecular formula of  $(\text{Bu}_4\text{N})[\text{Mo}^{\text{V}}\text{O}(\text{2H-qpdt})_2]$  for **12**. The CV of **12** is shown in Figure S15. It displays a reversible wave at  $-0.51\text{ V}$  for the  $\text{Mo}^{\text{IV}} / \text{Mo}^{\text{V}}$  couple, and a quasi-reversible wave at  $+0.3\text{ V}$  corresponding to the  $\text{Mo}^{\text{V}} / \text{Mo}^{\text{VI}}$  transition. These potentials are more negative than those obtained for **11**, in full agreement with the increased electron density on the ligand. Furthermore, the  $E_{\text{oc}}$  (open circuit voltage) for **12** is at  $-0.46\text{ V}$ , more positive than the potential of the  $\text{Mo}^{\text{IV}} / \text{Mo}^{\text{V}}$  transition, suggesting that the Mo center has a formal oxidation state of  $+V$ . This observation is consistent with the UV-Vis absorption spectrum of **12** in  $\text{CH}_3\text{CN}$  (Figure S16) that displays two absorption bands at low energy (582 and 808 nm), reminiscent of those observed in the case of  $[\text{Mo}^{\text{V}}\text{O}(\text{dithiolene})_2]^-$  complexes,<sup>5c, 13b, 16</sup> and of dimethylsulfoxide reductase (DMSOR) from *Rhodobacter capsulatus*.<sup>17</sup> The presence of  $S=1/2\text{ Mo(V)}$  species is demonstrated by the  $g = 2$  signal observed in the EPR spectrum of complex **12** recorded at  $70\text{ K}$  characteristic of  $\text{Mo(V)OS}_4$  centers (Figure S17).<sup>18</sup> Consistently,  $^1\text{H}$  resonances associated with the ligand in the  $^1\text{H}$  NMR spectrum in  $\text{CD}_3\text{CN}$

(Figure S18) are broadened.<sup>13b</sup> Finally, in the absence of a crystal structure, we propose that complex **12** has its dithiolene ligand conformationally organized as in  $[\text{Co}^{\text{III}}\text{Cp}(\text{2H-qpdt})]$  (**10**) but cannot conclude whether the two dithiolenes are *cis*- or *trans*-oriented or both and Scheme 3 leaves this opened.

Catalytic  $\text{CO}_2$  reduction activity of complexes **11** and **12** was assessed under photochemical conditions. For comparison, we also included the previously reported  $(\text{Bu}_4\text{N})_2[\text{Mo}^{\text{IV}}\text{O}(\text{qpdt})_2]$  complex (**13**).<sup>6a</sup> The reaction conditions were defined according to the standard ones commonly developed by O. Ishitani and co-workers:  $[\text{Ru}(\text{bpy})_3]^{2+}$  was used as a photosensitizer (PS) with a [PS]:[cat] of 10:1, BIH (1,3-dimethyl-2-phenyl-2,3-dihydro-1H-benzimidazole) as the sacrificial electron donor and  $\text{CH}_3\text{CN}$ -TEOA (triethanolamine) in a 5:1 ratio as the solvent.<sup>19</sup> Lower proportions of TEOA ( $\text{CH}_3\text{CN}:\text{TEOA} = 9:1$ ) resulted in decreased activity and slightly larger proportions of  $\text{H}_2$  (Table S1). The reaction products ( $\text{CO}$ ,  $\text{H}_2$  and  $\text{HCOOH}$ ) were monitored during the course of the reaction. The results, in terms of Turnover Numbers (TONs) based on the catalyst after 15h, are summarized in Table 1. Blank experiments showed no formation of products in the absence of PS or when the reaction was carried out in the dark. Tiny amounts of formate,  $\text{CO}$  and  $\text{H}_2$  were detected in the absence of complex (Table S1), likely due to some degradation of  $[\text{Ru}(\text{bpy})_3]^{2+}$  into  $[\text{Ru}(\text{bpy})_2\text{L}_2]^{2+}$  ( $\text{L} = \text{solvent}$ ), known as a catalyst for the reduction of  $\text{CO}_2$ .<sup>20</sup> Even lower amounts of products were observed in the absence of BIH (Table S1).

The data in Table 1 clearly show that the three complexes were catalyzing catalyze  $\text{CO}_2$  photoreduction, however with competitive  $\text{H}^+$  reduction. While the largest total TON values were obtained with  $[\text{MoO}(\text{qpdt})_2]^{2-}$  (**13**) followed by complex **12** and finally complex **11**, much less active, **13** was mainly producing produces  $\text{H}_2$  (81%) together with a small proportion of  $\text{CO}$  (9%) and formate (10%). It is interesting to note that a pyrazine-dithiolate nickel complex was reported as an excellent catalyst for proton reduction, thanks to ligand-based proton-coupled electron-transfer pathways.<sup>21</sup> Complex **12** promoted promotes the formation of a much larger proportion of  $\text{CO}_2$ -derived products accounting for almost 60% (with 39% formate and 19%  $\text{CO}$ ), while complex **11** was intermediate (53 %  $\text{H}_2$ ). Thus the selectivity for  $\text{CO}_2$  reduction vs  $\text{H}^+$  reduction drastically increased increases from **13** (0.23) to **11** (0.86) and finally to the most biomimetic **12** (1.38).

**Table 1.** TONs of formate,  $\text{CO}$  and  $\text{H}_2$  after 15 hours irradiation with a 300 W Xe arc lamp equipped with a 400 nm filter at  $20\text{ }^\circ\text{C}$ . Each sample contains 0.05 mM of catalyst, 0.5 mM of  $[\text{Ru}(\text{bpy})_3]\text{Cl}_2$ , 0.1 M of BIH in 1 mL  $\text{CO}_2$ -saturated  $\text{CH}_3\text{CN}$ -TEOA (5:1, v/v) solvent mixture.

Cat.	HCOOH	CO	$\text{H}_2$	Selectivity $\text{CO}_2/\text{H}^+$
<b>13</b>	80	73	670	0.23
<b>11</b>	31	13	51	0.86
<b>12</b>	83	40	89	1.38

Figure 5 shows a time curve for  $\text{CO}_2$  photoreduction catalyzed by **12**. Formation of products is sustained during about 8 hours, producing more than 100 TONs (for  $\text{HCOOH} + \text{CO}$ ), after which a plateau was reached, very likely due to bleaching of the PS. As a confirmation, after 8 h of experiment, the

reaction was found to restart upon addition of a fresh solution of 0.5 mmol of  $[\text{Ru}(\text{bpy})_3]\text{Cl}_2$ . After additional 15 hours of irradiation, 188/135/150 TONs were found for  $\text{HCOOH}/\text{CO}/\text{H}_2$  respectively (Figure S19). Finally, contribution of Mo particles was excluded based on a mercury test (Figure S20).

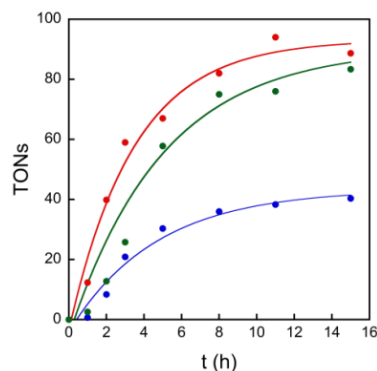


**Figure 5.** TONs of formate (●), CO (●) and H<sub>2</sub> (●) as function of time during irradiation of a CO<sub>2</sub>-saturated CH<sub>3</sub>CN/TEOA (5:1 v/v) solution (1 mL) containing 0.05 mM of **12**, 0.5 mM of Ru(bpy)<sub>3</sub><sup>2+</sup> and 0.1 M of BIH.

In conclusion, we here report not only the closest first relevant synthetic mimick model of the active site of FDHs but also the first bis-dithiolene-Mo complex displaying catalytic activity for CO<sub>2</sub> reduction. It is one of the very rare molecular catalysts generating formate as the major CO<sub>2</sub> reduction product under photoactivation conditions, together with the Mn(diimine)(CO)<sub>3</sub>X and the Rh(Cp)(diimine)X complex families.<sup>22</sup> In terms of TONs, it compares well with them, but needs to be further optimized with respect to the CO<sub>2</sub>/H<sub>2</sub> reduction selectivity. With such a structural and functional similarity to FDH active center, it provides a novel perspective for better understanding the functional specificity of that center, for making further progress towards even more biomimetic catalysts (in particular mimicking the axial ligation), for understanding reaction mechanisms and finally for discovering more selective bioinspired catalysts for CO<sub>2</sub> reduction.

## Acknowledgements

We acknowledge support from the French National Research Agency (ANR, PhotoCarb ANR-16-CE05-0025-01; Grant "Labex DYNAMO" ANR-11-LABX-0011). We thank Nadia Touati (Chimie ParisTech) and Hemlata Agarwala for the EPR measurements.

**Keywords:** Dithiolene ligands • Molybdenum complex • CO<sub>2</sub> reduction • Homogeneous catalysis

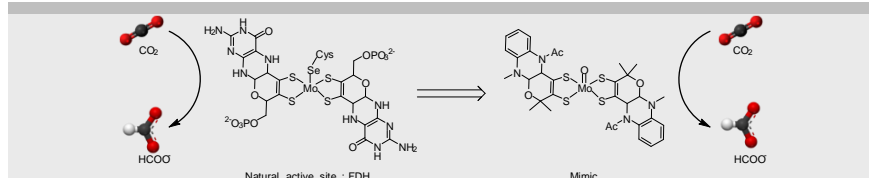
- [1] A. S. Agarwal, Y. Zhai, D. Hill, N. Sridhar, *ChemSusChem* **2011**, *4*, 1301-1310.  
 [2] a) M. J. Romao, *Dalton Trans.* **2009**, 4053-4068; b) L. B. Maia, J. J. G. Moura, I. Moura, *J. Biol. Inorg. Chem.* **2015**, *20*, 287-309.  
 [3] a) B. Bradshaw, D. Collison, C. D. Garner, J. A. Joule, *Chem. Commun.* **2001**, 123-124; b) B. Bradshaw, A. Dinsmore, W. Ajana, D. Collison, C. D. Garner, J. A. Joule, *J. Chem. Soc. Perkin Trans. 1* **2001**, 3239-3244; c) L. Marbella, B. Serli-Mitasev, P. Basu, *Angew. Chem. Int. Ed.* **2009**, *48*, 3996-3998; d) P. Basu, I. Pimkov, *U.S. Pat. Appl. Publ.*, US 20120245168 A1 20120927 **2012**.

- [4] a) B. R. Williams, Y. C. Fu, G. P. A. Yap, S. J. N. Burgmayer, *J. Am. Chem. Soc.* **2012**, *134*, 19584-19587; b) B. R. Williams, D. Gisewhite, A. Kalinsky, A. Esmail, S. J. N. Burgmayer, *Inorg. Chem.* **2015**, *54*, 8214-8222.  
 [5] a) J. H. Enemark, J. J. A. Cooney, J.-J. Wang, R. H. Holm, *Chem. Rev.* **2004**, *104*, 1175-1200; b) S. Groysman, R. H. Holm, *Inorg. Chem.* **2007**, *46*, 4090-4102; c) B. S. Lim, J. P. Donahue, R. H. Holm, *Inorg. Chem.* **2000**, *39*, 263-273; d) P. Basu, S. J. N. Burgmayer, *J. Biol. Inorg. Chem.* **2015**, *20*, 373-383; e) C. Schulzke, *Eur. J. Inorg. Chem.* **2011**, 1189-1199; f) H. Sugimoto, H. Tsukube, *Chem. Soc. Rev.* **2008**, *37*, 2609-2619; g) A. Majumdar, S. Sarkar, *Coord. Chem. Rev.* **2011**, *255*, 1039-1054.  
 [6] a) J. P. Porcher, T. Fogeron, M. Gomez-Mingot, E. Derat, L. M. Chamoreau, Y. Li, M. Fontecave, *Angew. Chem. Int. Ed.* **2015**, *54*, 14090-14093; b) J. P. Porcher, T. Fogeron, M. Gomez-Mingot, L. M. Chamoreau, Y. Li, M. Fontecave, *Chem. Eur. J.* **2016**, *22*, 4447-4453; c) T. Fogeron, J.-P. Porcher, M. Gomez-Mingot, T. K. Todorova, L.-M. 13Chamoreau, C. Mellot-Draznieks, Y. Li, M. Fontecave, *Dalton Trans.* **2016**, *45*, 14754-14763; d) T. Fogeron, T. K. Todorova, J. P. Porcher, M. Gomez-Mingot, L. M. Chamoreau, C. Mellot-Draznieks, Y. Li, M. Fontecave, *ACS Catal.* **2018**, *8*, 2030-2038.  
 [7] M. Jormakka, S. Törnroth, B. Byrne, S. Iwata, *Science* **2002**, *295*, 1863-1868.  
 [8] a) R. A. Rothery, B. Stein, M. Solomonson, M. L. Kirk, J. H. Weiner, *PNAS* **2012**, *109*, 14773-14778; b) H. Adamson, A. N. Simonov, M. Kierzek, R. A. Rothery, J. H. Weiner, A. M. Bond, A. Parkin, *PNAS* **2015**, *112*, 14506-14511; c) M. G. Bertero, R. A. Rothery, M. Palak, C. Hou, D. Lim, F. Blasco, J. H. Weiner, N. C. J. Strynadka, *Nat. Struct. Biol.* **2003**, *10*, 681-687; d) C. C. Lee, N. S. Sickerman, Y. L. Hu, M. W. Ribbe, *ChemBioChem* **2016**, *17*, 453-455.  
 [9] F. A. Alphonse, R. Karim, C. Cano-Soumillac, M. Hebray, D. Collison, C. D. Garner, J. A. Joule, *Tetrahedron* **2005**, *61*, 11010-11019.  
 [10] a) R. F. Heck, *Inorg. Chem.* **1965**, *4*, 855-857; b) R. B. King, *Inorg. Chem.* **1966**, *5*, 82-87.  
 [11] M. Fourmigue, *Coord. Chem. Rev.* **1998**, *178*, 823-864.  
 [12] M. Nomura, *Dalton Trans.* **2011**, *40*, 2112-2140.  
 [13] a) J. P. Smit, W. Purcell, A. Roodt, J. G. Leipoldt, *Polyhedron* **1993**, *12*, 2271-2277; b) E. S. Davies, R. L. Beddoes, D. Collison, A. Dinsmore, A. Docrat, J. A. Joule, C. R. Wilson, C. D. Garner, *J. Chem. Soc. Dalton Trans.* **1997**, 3985-3995; c) A. Doring, C. Fischer, C. Schulzke, *J. Anorg. Allg. Chem.* **2013**, *639*, 1552-1558.  
 [14] a) A. C. Ghosh, P. P. Samuel, C. Schulzke, *Dalton Trans.* **2017**, *46*, 7523-7533; b) P. P. Samuel, S. Horn, A. Doring, K. G. V. Havelius, S. Reschke, S. Leimkuhler, M. Haumann, C. Schulzke, *Eur. J. Inorg. Chem.* **2011**, 4387-4399.  
 [15] D. Coucouvanis, A. Hadjikyriacou, A. Toupadakis, S. M. Koo, O. Ieperuma, M. Draganjac, A. Salifoglou, *Inorg. Chem.* **1991**, *30*, 754-767.  
 [16] R. L. McNaughton, M. E. Helton, N. D. Rubie, M. L. Kirk, *Inorg. Chem.* **2000**, *39*, 4386-4387.  
 [17] B. Adams, A. T. Smith, S. Bailey, A. G. McEwan, R. C. Bray, *Biochemistry* **1999**, *38*, 8501-8511.  
 [18] Young, C. G., *J. Inorg. Biochem.* **2016**, *162*, 238-252.  
 [19] Y. Tamaki, K. Koike, T. Morimoto, O. Ishitani, *J. Catal.* **2013**, *304*, 22-28.  
 [20] J. Hawecker, J.-M. Lehn, R. Ziessel, *J. Chem. Soc. Chem. Commun.* **1985**, 56-58.  
 [21] Koshiha, K.; Yamauchi, K.; Sakai, K., *Angew. Chem. Int. Ed.* **2017**, *56*, 4247-4251.  
 [22] a) N. Elgrishi, M. B. Chambers, X. Wang, M. Fontecave, *Chem. Soc. Rev.* **2017**, *46*, 761-796; b) H. Takeda, C. Cometto, O. Ishitani, M. Robert, *ACS Catal.* **2017**, *7*, 70-88.

## Entry for the Table of Contents

Layout 2:

## COMMUNICATION



*T. Fogeron, P. Retailleau, L.-M. Chamoreau, Y. Li\*, M. Fontecave\**

**Page No. – Page No.**

**Pyranopterin Related Dithiolene Molybdenum Complexes as Homogeneous Catalysts for CO<sub>2</sub> Photoreduction**

Two original dithiolenes, mimicking molybdopterin (MPT) present in the active site of formate dehydrogenases (FDHs), have been synthesized and characterized. MoO(dithiolene)<sub>2</sub> complexes have been also prepared and are reported as the first functional and stable catalysts inspired by the Mo center of FDHs: they indeed catalyze the photoreduction of CO<sub>2</sub> into formic acid as the major product.